



Effects of Superhydrophobic, Hydrophobic and Hybrid Surfaces in Condensation Heat Transfer

H. Davar, N. M. Nouri[†] and M. Navidbakhsh

School of Mechanical Engineering, Iran University of Science and Technology, Tehran, 16846-13114, Iran

[†]Corresponding Author Email: mnouri@iust.ac.ir

(Received May 19, 2020; accepted December 25, 2020)

ABSTRACT

The effects of different hydrophobic and superhydrophobic coatings of PDMS, TGIC, SiO₂ and a commercial coating called Danphobix on the condensation heat transfer characteristics of the plates were investigated and compared with the uncoated surface. The initial investigation showed that the values of heat flux and condensation heat transfer coefficient of the plate with Danphobix coating are higher than other coatings. Then, the plates with the commercial coating Danphobix were investigated at five different thicknesses to enhance the condensation heat transfer coefficient. Scanning Electron Microscopy analysis of surface with Danphobix coating showed that the hydrophilic-hydrophobic parts of the generated hybrid surface are formed irregularly in a new intertwined manner. According to the obtained results, decreasing the initial thickness of coating to a definite value, the condensation heat transfer coefficient was augmented. By further decrease, the condensation heat transfer coefficient was reduced due to the elimination of the physical structures of the coating against steam. The highest values of condensation heat transfer coefficient and heat flux of plates with Danphobix coating, that was obtained at the coating thickness of 17 μm comprised 65.2% of the surface coating by Danphobix. The results indicated that the heat flux and condensation heat transfer coefficient values of the plate with Danphobix coating thickness of 17 μm was increased by 1.97-2.14 times and 1.96-2.46 times compared to the non-coated plate, respectively. In what follows, in addition to the critical thickness, the critical area of the coated surface is also obtained.

Keywords: Dropwise condensation; Heat flux; Condensation heat transfer coefficient; Hybrid hydrophobic-hydrophilic surface.

NOMENCLATURE

A	condensing surface area	T_i	thermocouple position temperature
A_{Coat}	percentage of surface coated	T_{in}	inlet water temperature
$c_{p,l}$	specific heat of water	T_{out}	outlet water temperature
\dot{m}	mass flow rate of water in condenser	T_s	steam temperature
$CHTC$	Condensation heat transfer coefficient	T_w	surface temperature
h_{fg}	latent heat of vaporization	ΔT	subcooling temperature, $(T_s - T_w)$
Δl	distance	u_A	type-A uncertainty
M	mass of condensate from the test plate	u_B	type-B uncertainty
Q	heat transfer rate	u_C	combined uncertainty
q	heat flux	u_M	expanded uncertainty
t	experimental time	u_{tot}	global uncertainty
k	thermal conductivity		

1. INTRODUCTION

Condensation is one of the central heat transfer regimes, which has been widely used in many industries, namely power generation industries (Beér 2007), heating ventilation and air

conditioning (Liu and Jacobi 2006), chemical production (Khawaji *et al.* 2008), and electronics thermal management (Peters *et al.* 2012).

Schmidt *et al.* (1930) showed that the condensation heat transfer coefficient (CHTC) at the droplet condensation is about 5-6.2 times that of the film

condensation, which then led dropwise condensation to cut the attention of many researchers.

Many researchers, including Citakoglu and Rose (1968), Izumi *et al.* (2004), and Koch *et al.* (1997), reported higher rates of water vapor condensation on vertical beds at a definite condensation degree. Koch *et al.* (1997) reported a relation for the CHTC in dropwise condensation as a function of bed slope and showed that the highest value of heat transfer was met on vertical plates and reduced by increasing the slope angle. Majumdar and Mezig (1999) experimentally investigated the performance of compressed steam condensers, showing that the condenser performance was enhanced after using specific chemicals with the width of a few millimeters as the hydrophobizing coating at the flow passage. Vemuri and Kim (2006) experimentally performed a condensation test on different coating surfaces using low-energy-level materials and reported the long-term stability of dropwise condensation and enhancement of CHTC. Testers coated a copper surface with one-layer, N-octadecyl mercaptan, and stearic acid coatings. The CHTC was reported three times that of the non-modified plain copper surface. Tianqing *et al.* (2007) experimentally illustrated that on-surface condensation initiation was not dropwise and filmwise from the very beginning. Their results revealed that the formation mechanism of initial droplets for dropwise condensation has been based on the theory of nucleation sites. Accordingly, most of the recent analytical models have been developed assuming the formation of droplets at nucleation sites, condensation process on free surface of droplets per se, negligible heat transfer between droplets, and latent heat transfer through droplets towards the solid surface. Baojin *et al.* (2011) performed an experimental study to calculate condensation heat transfer on a vertical titanium plate with different energy levels. They demonstrated that the calculation results of higher-energy-level plate heat transfer were consistent with the Nusselt theory. The values of heat flux of dropwise condensation on a plate with hydrophobic surface was 2.8-4.7 times compared to filmwise condensation on a plate with hydrophilic surface, in subcooling temperature 2-12 °C.

Parin *et al.* (2016) compared the condensations on an aluminum superhydrophobic plate with fluorosilane coating and on a coating-less aluminum hydrophilic plate for reducing the surface energy and revealed that the CHTC of the superhydrophobic plate was about four times higher as compared to a hydrophilic untreated aluminum sample.

Ghosh *et al.* (2014) examined various hydrophilic-superhydrophilic patterns, which combine and sustain filmwise condensation and DWC on the substrate, respectively. They found a special pattern of hydrophilic-superhydrophilic surface called bioinspired interdigitated pattern that performed better compared to the straight hydrophilic-superhydrophilic pattern design under

higher humidity conditions in the presence of noncondensable gases.

Nevertheless, the conjunction of superhydrophobic and superhydrophilic features on surfaces has been of great interest to many researchers over the past years. If one can create specifically patterned and designed roughness on a high-energy-level surface (hydrophilic), a surface with the hydrophobic-hydrophilic conjunction feature can be reached. For instance, nano-scale roughness can be created on surfaces such as copper, aluminum, titanium, and zinc that are intrinsically hydrophilic by the cell-gel method, anodizing method, or other methods to provide the hydrophobic feature. In the case of condensation on such surfaces, water droplets form swiftly due to the hydrophilic feature and liquid droplets separate from each other due to the hydrophobic feature, avoiding the formation of a liquid film. Peng *et al.* (2015) experimentally investigated the steam condensation heat transfer increase on hydrophobic-hydrophilic hybrid vertical plates. They revealed that the condensation heat transfer performance on these hybrid surfaces improves at first by increasing the width of hydrophobic section to a definite value and after which it decreases, leading to an optimum width for hydrophilic surfaces. They showed that steam condensation heat transfer using well-designed combined hydrophilic-hydrophobic surfaces can progress more easily and effectively. Peng *et al.* (2014) indicated also that the filmwise and dropwise hybrid surface can be effectively applied to enhance the condensation heat transfer of steam for the condensing surface with larger contact angle hysteresis or smaller contact angle and under low surface subcooling degree. They also showed that the condensation performance on hydrophobic-hydrophilic hybrid plates increased compared to fully hydrophobic plates. Ji *et al.* (2019) experimentally investigated dropwise condensation heat transfer on superhydrophilic-hydrophobic network hybrid surface. Three kinds of superhydrophilic-hydrophobic surfaces were tested, having a grid spacing of 1.5, 2.5 and 3.5 mm. The results show that superhydrophilic-hydrophobic surface can well control condensate droplet diameters and its condensation heat transfer performance is better than that of smooth hydrophilic and hydrophobic surfaces. The Maximum amount of heat transfer coefficient of superhydrophilic-hydrophobic-2 surface was 2.7 and 3.4 times that of hydrophilic and hydrophobic surfaces, respectively.

Oestreich *et al.* (2019) experimentally discussed the effect of hydrophilic constructal-like patterns on the condensate mass flow rate production of superhydrophobic vertical test sections. They tested five different designs, three with a branched topology having coated/clear area fractions of approximately 30%, 50% and 70%, in addition to fully clear and fully coated test sections. According to the results, slightly higher condensation rates were obtained for some of the experimental sections which covered 70% of its surface area with a superhydrophobic layer. Ansari (2017)

hydrophobized alumina, silica, and phlogopite micro/nano powders by the steam method and deposited them with proper resin on an aluminum surface by the electrostatic method. In this method, the concerned powder which is chemically ready to be bonded with hydrophobic substances is placed in a controlled chamber adjacent to the steam of hydrophobic substance for sufficient bonding time. Then, the prepared powders are put in a furnace to produce super-hydrophobic powders. The prepared powders are mixed with a definite percentage of powder resin such as TGIC and placed on the surface by the electrostatic method. The hydrophobic angle of surfaces was measured as ranging between 167° and 171° . These surfaces were used for an antifouling test where the primary test results suggested their appropriate performance.

Derby et al. (2014) surveyed the flow condensation of steam in the hydrophilic-hydrophobic hybrid microchannels. According to the results obtained, the steam condensation heat transfer coefficient for the hydrophobic and hydrophilic-hydrophobic patterned channels could surpass that of the hydrophilic surface by an order of magnitude. *Chatterjee et al. (2013)* illustrated that steam CHTC on a surface with island patterns of hydrophobic and hydrophilic regions were lower than that of the hydrophobic surface and higher than that of the hydrophilic surface. The influence of feature size and shape of pattern (tree pattern and island pattern) on steam CHTC was also experimentally measured (*Chatterjee et al. 2014*).

Despite the positive effects of using hybrid surfaces instead of fully hydrophobic surfaces, examining the fabrication of plates with hybrid surfaces in the work performed shows the high cost of producing a hybrid surface. Efforts to reduce the cost of producing hybrid surfaces are of paramount importance.

In the present study, different hydrophobic and super-hydrophobic surfaces are produced and coated by different methods such as the electrostatic coating technique. Moreover, new hybrid hydrophilic-hydrophobic surfaces are generated by the electrostatic method and the CHTC induced by the dropwise condensation on these surfaces is evaluated. The key point is that most hybrid hydrophilic-hydrophobic surfaces have specific geometric shapes. In other words, the hydrophilic part is generated on the plates as grid/direct lines with definite depth and thickness. The optimal values of thickness and depth are obtained by experimental tests and the production of these surfaces entails high costs and is time-consuming. In this study, the hydrophilic-hydrophobic parts of the generated hybrid surface are formed irregularly in an intertwined manner. Generating the hybrid surface introduced in this article was cheaper and easier than the hybrid levels of other articles. Usually, the work done in the field of hydrophobic surfaces is limited to the laboratory scale, while the surface with Danphobix coating can be used on a large scale. Most hydrophilic-hydrophobic hybrid surfaces are made in several steps, while the

Danphobix coating is made in one step. Due to the fact that no toxic solvents such as toluene and acetone have been used in the manufacture of Danphobix coating, this coating is considered as an environmentally friendly coating.

Moreover, the effects of this coating on the condensation were assessed as well.

2. EXPERIMENTS INTRODUCTION

The condensation experiments were conducted in a condensation chamber, specifically built for these experiments. The primary purposes of the experiments are investigating the effects of different coatings and different thicknesses of Danphobix coating on condensation heat transfer characteristics such as heat flux and CHTC.

2.1 Materials

Al-3003 was purchased from the Iranian Aluminum Company. All reagents were of analytical grade, including Trichloromethylsilane (TCMS) (99.9%), acetone (99.9%) and deionized water (DIW) were purchased from Merck Chemicals and used without further purification. Danphobix was made in the Institute of Applied Hydrodynamics and marine technology of Iran University of Science and Technology (Hydrotechei) and the particle diameter is 40-120 μm . Sylgard 184, a Polydimethylsiloxane (PDMS), was supplied by Dow Corning. Hydrophobic Silicon dioxide (SiO_2) nano particle, with an average diameter of ~ 20 nm, was kindly provided by US nano research. Polyester, a Triglycidylisocyanurate (TGIC), with a diameter of 50 μm was kindly provided by Bajac Co, Tehran, Iran.

2.2 Experimental Apparatus

To obtain the aforementioned parameters in the previous section, experimental equipment should be provided, namely steam generation system, cooling system, steam condensation system, and information control system, as shown in the following figure. Distilled water was directed to a steam generator by a diaphragm pump. Due to the absence of a propeller, this type of pump was resistant to cavitation, produced slight vibrations, and generated low-value stresses with fluid. 100°C steam was produced by the steam generator. Then, the produced steam passed through a super-heater for the sake of transparency and clarity. The dry steam was directed to the condensing chamber through a channel and condensate over the condensation test plate. The steam velocity in the channel was calculated by dividing the volumetric flow rate into the channel cross-sectional area. The steam temperature was measured by a platinum resistance thermometer (Pt 100) with the error of $\pm 0.1^\circ\text{C}$. This thermometer is a type of RTD which desired for the temperature range of -40 to 400°C . Resistance variations in terms of temperature are $0.365 \text{ Ohm}/^\circ\text{C}$.

To measure the temperature of intake cooling water, hot water exiting from the plate cooling chamber,

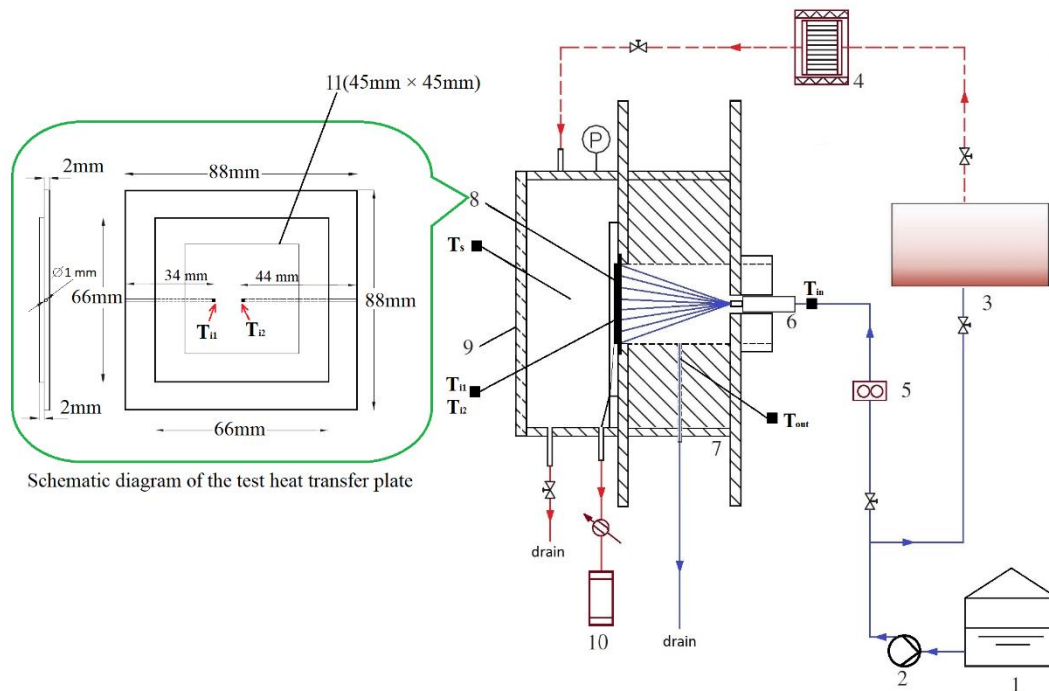


Fig. 1. Schematic diagram of the experimental apparatus. 1-Deionized water tank; 2- diaphragm pump; 3-steam generator; 4-superheater; 5- rotameter; 6-Water spray nozzle; 7-test section; 8- heat transfer plate; 9- glass window; 10- measuring tube, 11- Area of plate in contact with steam. ■ Temperature measuring position; — water line; - - - - steam line.

and vapor entering the condensing chamber, all three RTD thermometers were connected to the SU_105PRR model thermostats of SAMWON ENG Company with PT100Ω sensor with the temperature range of $-200+400^{\circ}\text{C}$, and the temperature of thermometers was displayed on the screens of these thermostats at any given time. On the other hand, two K-type thermocouples for measuring the temperature of condensing plate were connected to the SU-105KRR model thermostats of SAMWON ENG Company with K(CA) sensor with the temperature range of $-200+999^{\circ}\text{C}$, and the plate temperatures were displayed on these thermostats in any given time. Steam pressure was investigated by a manometer with the precision of millibar and was adjusted at atmospheric pressure by a valve installed at the end of the condensing chamber. A protector plate was installed all around the condensing plate to eliminate the effects of sweeping steam flow over condensate droplets. The condensate on the test plate was collected by a funnel, followed by being flowed into a measuring tube. The condensing chamber wall was fabricated of transparent Plexi with the width of 100mm and was provided to monitor the condensation process. To reduce the occurrence of the condensation process at other places of the chamber, rock wool insulator with the thickness of 50 mm was utilized. Accordingly, the effects of unwanted condensation were dramatically restricted and its effects on the pressure inside the chamber could be disregarded in experiments. The additional steam and condensate substances were collected on other surfaces of the condensing chamber by a measuring tube. Water

was employed to cool the plate and was kept in a cooling-water tank at a constant temperature. It was sprayed on the back of the test plate by a nozzle and a pump after being passed through a flow-meter. The heat flux of the heat transfer plate was regularly and constantly supplied by adjusting the pressure and cooling water flux. The effect of non-condensable gas is one of the most important parameters affecting condensation. This article is a study of condensation without the presence of non-condensable gas. For this reason, before saving the test data and during the warm-up period, the steam rapidly flowed through the condensing chamber for 60 min to eliminate the effect of non-condensing gas on heat transfer.

2.3 Heat Transfer Plate

Details of the test heat transfer plate are shown in Fig. 1. An aluminum square plate with the thickness of 4mm and dimensions of 88 mm×88 mm has been cut and two holes with the depths of 44mm and 34mm have been drilled into either side the plate to plant thermocouples with the diameter of 1mm to measure the plate temperature. Two Type K (NiCr-Ni) thermocouples were put into two holes to measure the wall temperature of plates. The temperature range of this type of thermocouple is $-250+1000^{\circ}\text{C}$ and its sensitivity is $46 \mu\text{V}/^{\circ}\text{C}$. This type of thermocouple is relatively cheap, applicable for low-temperature cases, and appropriately resistance to humidity. K-type thermocouple has the temperature measuring error of $\pm 0.1^{\circ}\text{C}$. The front part of the aluminum plate had the dimensions of 66 mm×66 mm and thickness of 2 mm, over which there is an area with the dimensions of 45

mm×45 mm where the condensation occurs on it, in contact with the steam and it is the same for the coated and uncoated surfaces. This area as shown in Fig.1, point.11.

2.4 Preparation of Samples

Due to the necessity for accurate and identical comparison of contact angle and CHTC between the surfaces with hydrophobic and superhydrophobic coatings, all of the surfaces have been fabricated with the coating width of $38 \pm 2 \mu\text{m}$. All surfaces were prepared in Hydrotechei:

Surface 1: Plain surfaces (No coating)

Surface 2: Firstly, to degreasing and cleaning fat and contamination from the surface, the Aluminum plate was washed with acetone. Then, the preparation process was conducted by the sandblast mechanical method. Then, the sandblasted surface was coated with the commercial powder Danphobix with electrostatic spraying method.

In the electrostatic spray, uniformity of combination of resin and additive microparticle is important factors in hydrophobic surface fabrication. The composite was put in a high-voltage electrostatic gun with 100-kV positive DC voltage. The distance between the aluminum substrates and gun was 15 cm. The whole substrate was sprayed to get covered by powders. As some of the powders were distributed in the air, substrate could not be coated by them. Hence, more mixed powders should be placed in the electrostatic container vessel in comparison to what is needed for coating. Given amount of powder depending on the coating condition is achieved regarding the experiments which is about 0.05 g/cm^2 to cover the whole surface. Then, coated samples put in an oven and warm up at temperature 300°C for 10 min. The most important parameters for controlling the thickness of the Danphobix coating are the distance between the gun and substrates, adjusting the pressure and the flow rate of the powder from the gun. (Danphobix-sandblast) *Surface 3:* Except for the sandblasting step, all the steps described in Surface 2 are performed. (Danphobix)

Surface 4 and 5: Firstly, to degreasing and cleaning fat and contamination from the surface, the Aluminum plate was washed with acetone. Then, PDMS was mixed in toluene and placed on the magnet stirrer for 15 minutes. Nano-silica materials were added to the solution and it was soaked in an ultrasonic bath for 30 minutes so that agglomerate particles were separated from each other. Then, proportional to the amount of polymer, the hardener was added. Subsequently, the coating process was performed by the aid of air pressure and the product was placed in the radiation furnace for 60 minutes at 100°C . The weight ratios of PDMS to SiO_2 in surfaces No.4 and No.5 were 1:1 and 1:9, respectively. (PDMS/ SiO_2 1:1 & PDMS/ SiO_2 1:9) *Surfaces 6 and 7:* Powder of SiO_2 nanoparticles were hydrophobized on micro and nano scales by the steam method and coated with proper resin on the surface by the electrostatic method. In this

method, the concerned powder -that was chemically ready to be bonded with hydrophobic materials- was placed in the controlled chamber close to the vapor of hydrophobic trimethylchlorosilane for sufficient time to be bonded. Then, the prepared powders were put in the furnace to become superhydrophobic. To remove fat and contamination from the surface, the Aluminum plate was washed with acetone. In this step, two types of plates were generated with different Si-to-resin weight ratios where the weight ratios of SiO_2 to TGIC polyester in surfaces No.6 and No.7 were 1:1 and 1:3, respectively. The coated surface was placed in the radiation furnace for 10 minutes at 200°C . (SiO_2/TGIC 1:1 & SiO_2/TGIC 1:3) *Surface 8:* The bottom of the aluminum base was directly coated, i.e. the surface was prepared at first by chemical methods such as boiling and sandblast. After sandblasting in the preparation stage, the washing process was performed for 20 minutes in acetone and 20 minutes in distilled water by the ultrasonic device. In this stage, initial roughness would be created over the surface. Then, trimethylchlorosilane (TCMS) was coated on the surface by the steam method under environmentally controlled conditions. Thus, the appropriate hierarchical roughness was generated for a superhydrophobic surface. After a definite time, the plate was put in the radiation furnace for 12 hours at 200°C . (Steam-Sandblast)

The amounts of thermal conductivity of coatings listed in Table 1.

2.5 Experimental Data Reduction

Two main parameters in the calculations of this stage include temperature of condensing plate T_w and heat flux q . The generated heat by the condensation on the condensing plate was transferred to the total cooling water behind the condensing plate. The condensation heat transfer rate was calculated by the following relation.

$$Q_1 = \frac{M \cdot h_{fg}}{t} \quad (1)$$

M is the mass of condensate water on the test plate. The heat transfer rate was calculated based on the mass flow rate and temperature increase in the cooling water by the following relation.

$$Q_2 = \dot{m} c_{p,l} (T_{out} - T_{in}) \quad (2)$$

Here, \dot{m} is the water mass flow rate inside the condenser. Q_1 was lower than Q_2 by 6%. Due to the imbalance in the amount of Q_1 and Q_2 , an average was taken into account between the upper and lower limits of these two values and, thus, the heat flux can be obtained by the following relation.

$$q = \frac{Q_1 + Q_2}{2A} \quad (3)$$

The averaged thermocouple position temperature

T_{i-ave} was obtained by the following relation.

Table 1 Amounts contact angle of coatings.

	No coating	Danphobix-sandblast	Danphobix	PDMS/SiO ₂ 1:1	PDMS/SiO ₂ 1:9	SiO ₂ /TGIC 1:1	SiO ₂ /TGIC 1:3	Steam-Sandblast
Thermal conductivity, k (W/m ² °C)	0	0.24	0.22	0.18	0.13	0.19	0.17	0.24
Contact angle (degree)	73±4	83±4	132±3	155±2	162±2	143±2	133±3	148±2
Contact angle hysteresis (degree)	-	-	~50	≤ 5	≤ 3	~11	~20	~9
Resin	-	Danphobix	Danphobix	PDMS	PDMS	TGIC polyester	TGIC polyester	-
Filler or Organosilane	-	-	-	Nano-silica	Nano-silica	Nano-silica	Nano-silica	TCMS
Weight percentage (filler/resin)	-	-	-	50	90	50	25	-
Sandblast	No	Yes	No	No	No	No	No	Yes
Coating methods	-	Electro-static	Electro-static	Spray	Spray	Electro-static	Electro-static	CVD

$$T_{i-ave} = \frac{T_{i1} + T_{i2}}{2} \quad (4)$$

T_{i1} and T_{i2} are thermocouple position temperatures that shown in Fig. 1.

The temperature of condensing surface T_w was obtained by the following relation regarding the calculated heat flux q and averaged thermocouple position temperature T_{i-ave} from the above relation.

$$T_w = T_{i-ave} + q \cdot \left(\frac{\Delta l_{Al}}{k_{Al}} + \frac{\Delta l_{coat}}{k_{coat}} \right) \quad (5)$$

Δl_{Al} stands for the distance between the aluminums surface and measuring points of the thermocouples located on the heat transfer plate. Δl_{Coat} is an equivalent thickness of coating which is calculated based on the coating coverage taken by SEM images to take coating thermal resistance into account in calculation of CHTC with considering coating coverage. k_{Al} and k_{Coat} are thermal conductivity of aluminums and coating, respectively. Moreover, the CHTC was obtained by the following relation:

$$HTC = \frac{q}{\Delta T} = \frac{q}{T_s - T_w} \quad (6)$$

2.6 Uncertainty Analysis

The experimental uncertainties are calculated following the general rules reported in ISO Guide to the Expression of Uncertainty in Measurement (1995). For each variable, the combined uncertainty u_C is calculated considering ‘‘Type A’’ and ‘‘Type B’’ components according to Eq. (7) and Eq. (8).

$$u_C(y) = \sqrt{\sum_{i=1}^n \left(\frac{df}{dx_i} \right)^2 u_{tot}^2(x_i)} \quad (7)$$

The global uncertainty of the measured data x_i is evaluated as

$$u_{tot}^2(x_i) = u_A^2(x_i) + u_B^2(x_i) \quad (8)$$

The uncertainty of the thermocouples position is assumed to be negligible. Where u_A(x_i) and u_B(x_i) are respectively the Type A and Type B uncertainties of the i-th variable x_i and n is the total number of measured variables.

Type A uncertainty is determined using the probability distribution of values of the observations was examined. Most frequently normal distribution is assumed while Type B uncertainty is related to the instrument properties and error propagation. In this regard, type A uncertainty of the measured variables such as mass, water flow rate and Temperatures is calculated according following Eq. (9).

$$u_A(x_i) = \frac{\sqrt{\sum_{j=1}^m \left(x_{i,j} - \frac{\sum_{j=1}^m x_{i,j}}{m} \right)^2}}{\sqrt{m-1}} \quad (9)$$

m represents the number of data recorded by the related sensor, which is currently equal to 10.

Instrument precision and related Type (B) uncertainty of the most measured variables are listed in Table 2. In this regard, according to Eq. (6),

the combined uncertainty of CHTC was obtained by Eq. (10).

$$u_c(HTC) = \sqrt{\left(\frac{\partial HTC}{\partial q}\right)^2 u_{tot}^2(q) + \left(\frac{\partial HTC}{\partial \Delta T}\right)^2 u_{tot}^2(\Delta T)} \quad (10)$$

q and ΔT are in depended variable which are calculated according to Eq. (11) and Eq. (12).

$$q = \frac{M \cdot h_{fg}}{2l^2 t} + \frac{\dot{m} c_{p,d} (T_{out} - T_{in})}{2l^2} \quad (11)$$

$$\Delta T = T_s - \frac{T_{i1} + T_{i2}}{2} - q \cdot \left(\frac{\Delta L_{Al}}{k_{Al}} - \frac{\Delta L_{Coat}}{k_{Coat}}\right) \quad (12)$$

The expanded uncertainty $u_M(x_i)$ is finally obtained by multiplying $u_c(x_i)$ by a coverage factor $k=2$. In this analysis, the uncertainties of the thermodynamic variables evaluated using NIST Refprop Version 9.1 (2013) are neglected.

According to the uncertainty propagation criterion, within the scope of the current experiments, the mean expanded uncertainties of the temperature difference between the steam, and the wall for all the data points, heat flux removed in the measuring section and CHTC are below than 3.5%, 4.5%, and 6.7% respectively.

2.7 Characterization

To measure both static contact angle and contact angle hysteresis, a Dataphysics OCA 15 Plus

instrument was utilized at room temperature ($25 \pm 1^\circ\text{C}$). Amount of 5 μL deionized, double-distilled water was used during the measurements. Number of 5 measurements were accomplished at 5 different points to obtain the contact angles for each sample. Surface of the samples were analyzed using scanning electron microscopy (SEM VEGA II XMU, Tescan Co., Czech). A thin Ag layer (5 nm) was deposited on the specimens, prior to SEM, to capture high quality images (Desk Sputter Coater DSR1, Nanostructured Coatings Co., Iran). Additionally, elemental analysis is done using energy-dispersive X-ray spectroscopy (EDX). The three-dimensional (3-D) topography of Danphobix films were obtained using optical profilometer (MOA-ZA, Fanavari Kahroba Co, Iran). Root mean square roughness (R_{rms}) values were determined by utilizing the data of surface profilometer.

3. RESULTS

3.1 Investigation into the Structures of Coatings on Surfaces by SEM and EDX

Figure 2 shows SEM images of surface structure for different hydrophobic and superhydrophobic surfaces. All of the surfaces were investigated at two magnifications of 1000x and 100x.

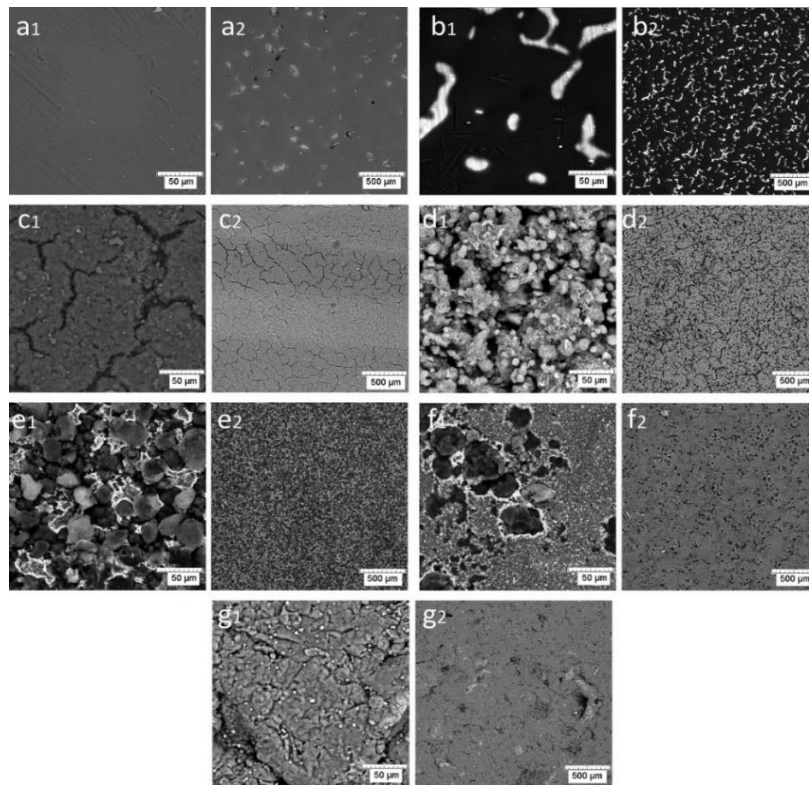


Fig. 2. SEM images: a1,a2= Danphobix-Sandblast, b1,b2= Danphobix, c1,c2= PDMS/SiO₂ 1:1, d1,d2= PDMS/SiO₂ 1:9, e1,e2= SiO₂/TGIC 1:1, f1,f2= SiO₂/TGIC 1:3, g1,g2= Steam- Sandblast.

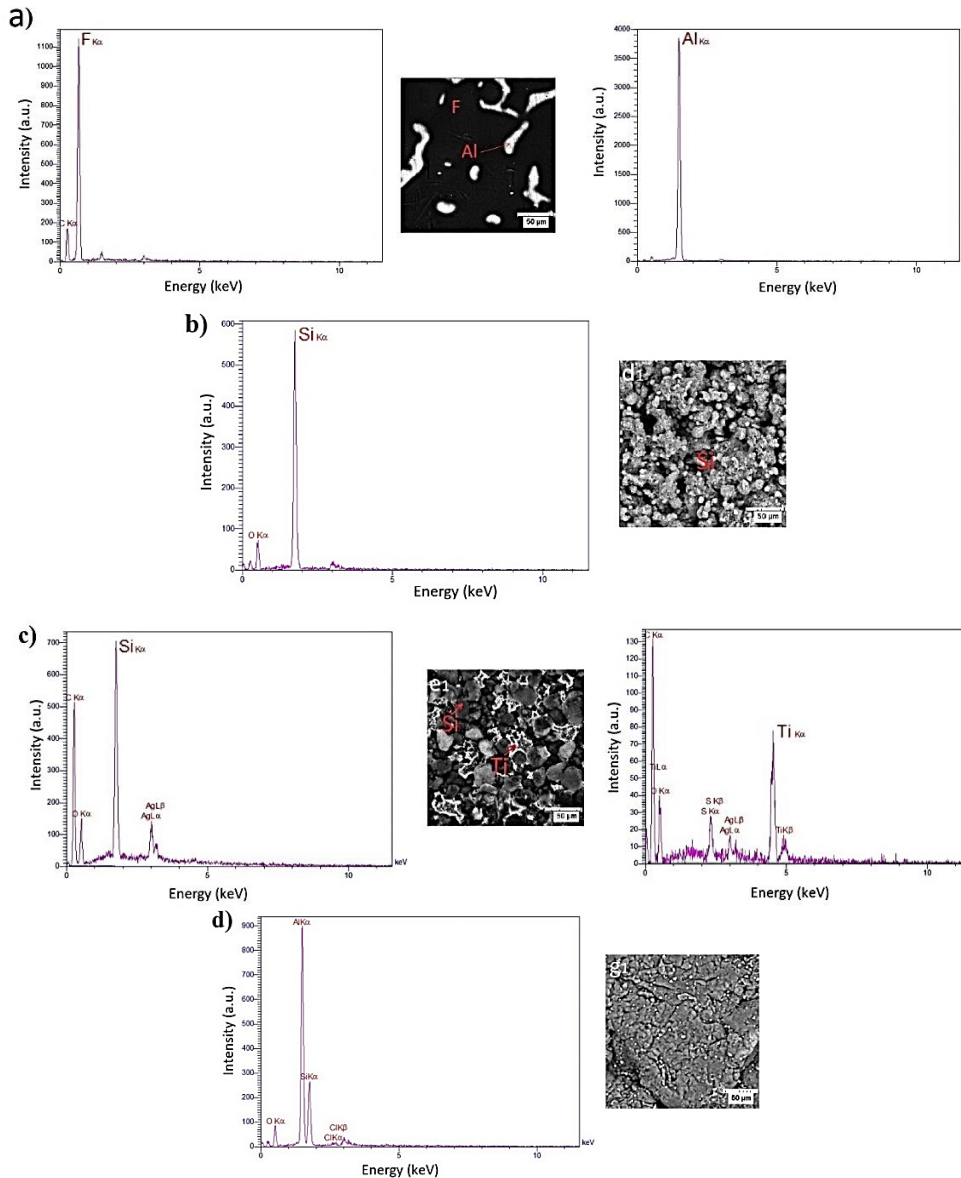


Fig. 3. EDX & SEM images of surface coating with: a=Danphobix, b= PDMS/SiO₂ 1:1, c= SiO₂/ TGIC 1:1 and d= Steam-sandblast.

Table 2 Type B uncertainty of the measured parameters.

Variable	Instrument precision $E(y)$	Uncertainty $u_B(y) =$ $E(y)/\sqrt{3}$
Temperature	± 0.05 K	0.03%
Cooling water flow rate	± 0.2 %	0.12%
Mass of condensate from the test plate (g)	± 0.05 g	0.03%
Thickness of coating	± 0.002 mm	0.001%
Thickness and length of plate	± 0.02 mm	0.01%
Time	± 0.01 s	0.01%

As it can be seen in Figs. 2. b₁ and 2. b₂, when the deposition of Danphobix particles on the aluminum substrate are placed in the furnace, a hydrophilic-hydrophobic structure is formed on the surface after

melting these particles. These structures indicate the polymer particles do not cover the entire surface while melting and it refers to the size of Danphobix particle, the way these particles are applied on

aluminum substrates (electrostatic spraying) and conditions related to the aluminum substrate (without the initial roughness by sandblasting). But unlike the structure of Danphobix-No sandblast surface, the structure of Danphobix- sandblast surface is completely coated by Danphobix particles, which is due to the roughness is created by the sandblast. Fig (2. a1, 2. a2).

Danphobix consists of Fluorocarbon compounds based on the EDX analysis indicated in Fig. 3.a. Figures 2. c1, 2. c2 and 2. d1, 2. d2 show the SEM images for the PDMS-SiO₂ coated with 50% and 10% PDMS/SiO₂ weight percentage, respectively. At low PDMS weight percentage, the surfaces show rough morphology. In this condition, the surface was coated with a thin layer of PDMS, making it possible to bond the microparticles. At high PDMS weight percentage, the surfaces exhibit a smooth morphology. Upon increasing the PDMS weight percentage to 50wt%, the surface pores were filled with PDMS and the surfaces roughness decreased.

The EDX analysis depicted in Fig. 3.b illustrates SiO₂ nanoparticles.

Figures 2. e1, 2. e2 and 2. f1, 2. f2 show the SEM images for the SiO₂- polyester (TGIC) coated with 25% and 50% SiO₂/polyester weight percentage, respectively. At low nano-particle content of 25 wt%, the coating surface is partly covered with nanoparticles (Fig. 2. e1, 2. e2).

As the nano-particle content increases to 50 wt%, more area will be covered by nano-particles (Fig. 2. f1, 2. f2). According to the EDX analysis shown in Fig. 3 .c, TGIC resin-polyester compounds are observed in addition to SiO₂ nanoparticles.

3.2 Condensation Parameters and Validation

First, the droplet contact angle with the surface was measured for all of the plates and compared to each other. In what follows, resistance of coating to water vapor, formation of condensation-induced droplets, CHTC and heat flux are investigated. The conducted measurements of contact angle and contact angle hysteresis are listed in Table 1.

Figure 4 also has shown a representative image of 5 μ L water droplet on the samples with Danphobix, SiO₂/TGIC 1:1 and PDMS/SiO₂ 1:1 coatings.

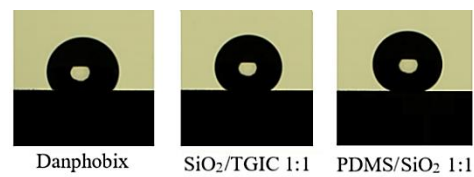


Fig. 4. Image of a 5 μ L water droplet on Danphobix, SiO₂/TGIC 1:1 and PDMS/SiO₂ 1:1 coated layers at same thicknesses (38 \pm 2 μ m).

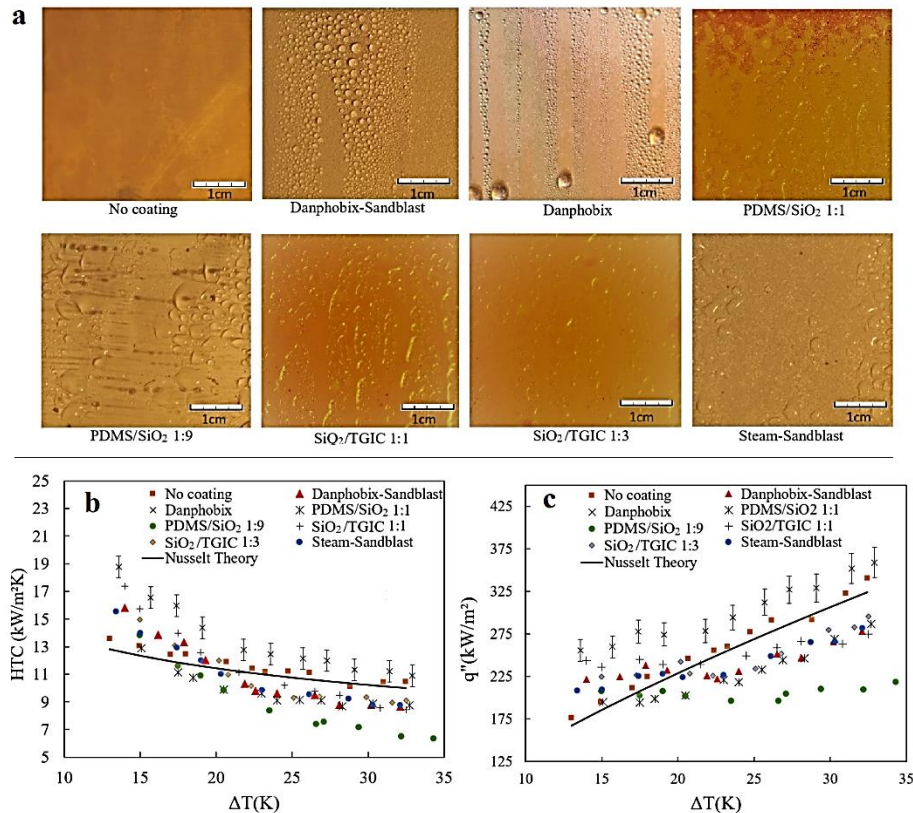


Fig. 5. Condensation on the different coated surfaces at same thicknesses (38 \pm 2 μ m); CHTC (b) and Heat flux (c) versus various subcooling temperatures over the different coated surfaces and Nusselt at same thicknesses (38 \pm 2 μ m).

According to the obtained results from the contact angle measurement, it was revealed that the plates with a superhydrophobic coating (SiO₂/TGIC 1:1 and PDMS/SiO₂ 1:9) offered lower contact angle hysteresis, higher contact angle and hydrophobicity compared to the plate without coating and other plates. Figure 5 depicts the formation of condensate droplet on each of the surfaces. The CHTC and heat flux values measured during condensation over the hydrophobic, hydrophilic and superhydrophobic treated aluminum substrate are reported in Fig. 5.b and Fig. 5.c, respectively. According to the laminar filmwise condensation on the vertical plate and using the assumptions based on the Nusselt analysis, the CHTC is expressed as follows for the entire plate (2003):

$$HTC = 0.943 \left[\frac{g \rho_l (\rho_l - \rho_v) k_l^3 (h_{fg} + 0.68 C_{p,l} (T_{sat} - T_w))}{\mu_l (T_{sat} - T_w) L} \right]^{\frac{1}{4}} \quad (13)$$

On the other hand, the CHTC in the filmwise condensation on a vertical aluminum plate was measured regarding the designed experimental setup, followed by a comparison between the two modes.

According to the obtained results, the CHTC obtained from the experimental values offered an acceptable error of ±6% relative to the Nusselt model. Therefore, the solutions obtained by the experimental tests were acceptably accurate.

By calculating CHTC and heat flux after each condensation test, the Danphobix-coated plate resulted in the highest values of CHTC and heat flux, as well as the best condensate droplet formation at this type of surface compared to other surfaces.

Trends are those expected during dropwise and filmwise condensation. The CHTC tends to decrease almost linearly when increasing subcooling temperature (ΔT). Instead, heat flux increases when increasing ΔT. Due to the detection of points in the figure, only the percentage of Danphobix coating error is shown, while the maximum error of all the data is taken into account, and the maximum is 7%.

It is worth noting, aside from Danphobix-Sandblast, Steam-Sandblast, and Danphobix coatings, the durability of physical structure of coatings vanished after 10 to 20 tests under steam condition and 15-35% of their CHTC is reduced.

In this respect, the durability of the Danphobix coating was not removed during 8 months and around 60 condensation tests but its CHTC was reduced by about 5%. Regarding the examination of CHTC and formation of condensation-induced droplets among the three mentioned coatings with high durability of physical structure, the Danphobix-coated offered more enhanced properties compared to other surfaces.

The most central index to select this coating in this stage was the formation process of the droplets induced by the dropwise condensation on the plate and invariability of physical properties.

The Danphobix coating benefited from the feature of inducing dropwise condensation on the plate, and the formation process of condensate droplets is illustrated in Fig. 5.a. On the other hand, the condensation on the non-coated aluminum plate occurred in the filmwise mode. According to the conducted investigations by researchers, the values of CHTC and heat flux were higher in the dropwise condensation than the filmwise one.

According to the given values in Fig. 5.b and Fig. 5.c, the values of CHTC and heat flux measured on the Danphobix-coated plate in the dropwise condensation has been larger than that on the non-coated plate in the filmwise condensation. The Danphobix coating thickness seemed to cause significant thermal resistance whereby the negative effect of this thermal resistance induced by the coating thickness was more dominant than the positive effect of forming dropwise condensation on the value of CHTC. Therefore, after selecting this surface as the appropriate surface for reducing the coating thickness, new plates were generated in the next stage to investigate the effect of thickness reduction on the value of CHTC.

3.3 Generation of New Plates

As already demonstrated in the previous section, the Danphobix-coated plate offered the best formation of condensate droplet compared to other surfaces. Furthermore, it provided the longest duration of durability against water vapor. Hence, five Danphobix-coated coatings were generated with different thicknesses.

By examining SEM images in Fig. 6 it was observed, increasing the coating thickness, a larger area of the plate was coated with Danphobix. In the following these five thicknesses were investigated in terms of contact angle, contact angle hysteresis and CHTC. Prior to performing the condensation test, the contact angle of droplets was examined and the amounts of droplet contact angle of coatings listed in Table 3.

In general, depending on the thickness of the coatings, two types of coatings can be considered. The first type of coatings are surfaces with Danphobix-Sandblast, PDMS/SiO₂ 1:1, PDMS/SiO₂ 1:9, SiO₂/TGIC 1:1, SiO₂/TGIC 1:3 and Steam-Sandblast coatings with 38μm thickness, which cover all area of the surface according to the examination of SEM photos (Fig. 2). The second type is Danphobix coating, which is made at different thicknesses (10 μm, 17 μm, 23 μm, 30 μm and 38 μm). According to SEM photos (Fig. 6), this coating does not cover the entire surface and some of the surface remains hydrophilic and uncoated. Therefore, an equivalent thickness (Δl_{Eq-coat}) is obtained.

depending on the amount of surface area covered by each surface and the Eq.(9).

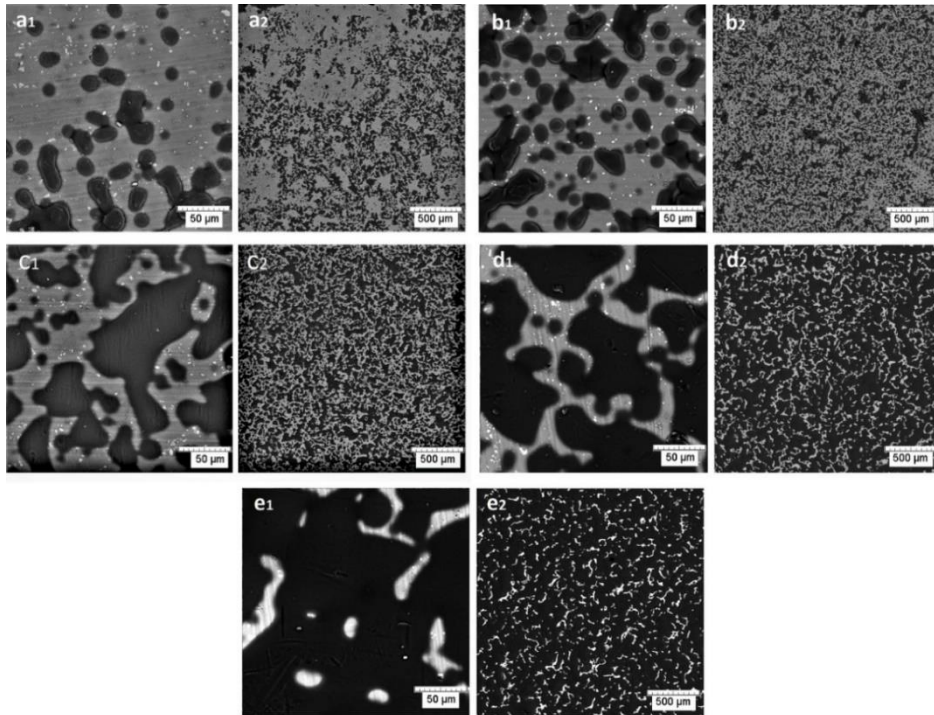


Fig. 6. SEM images with Danphobix coating; a₁,a₂= 10μm, b₁,b₂= 17μm, c₁,c₂= 23μm, d₁,d₂= 30μm, e₁,e₂= 38μm.

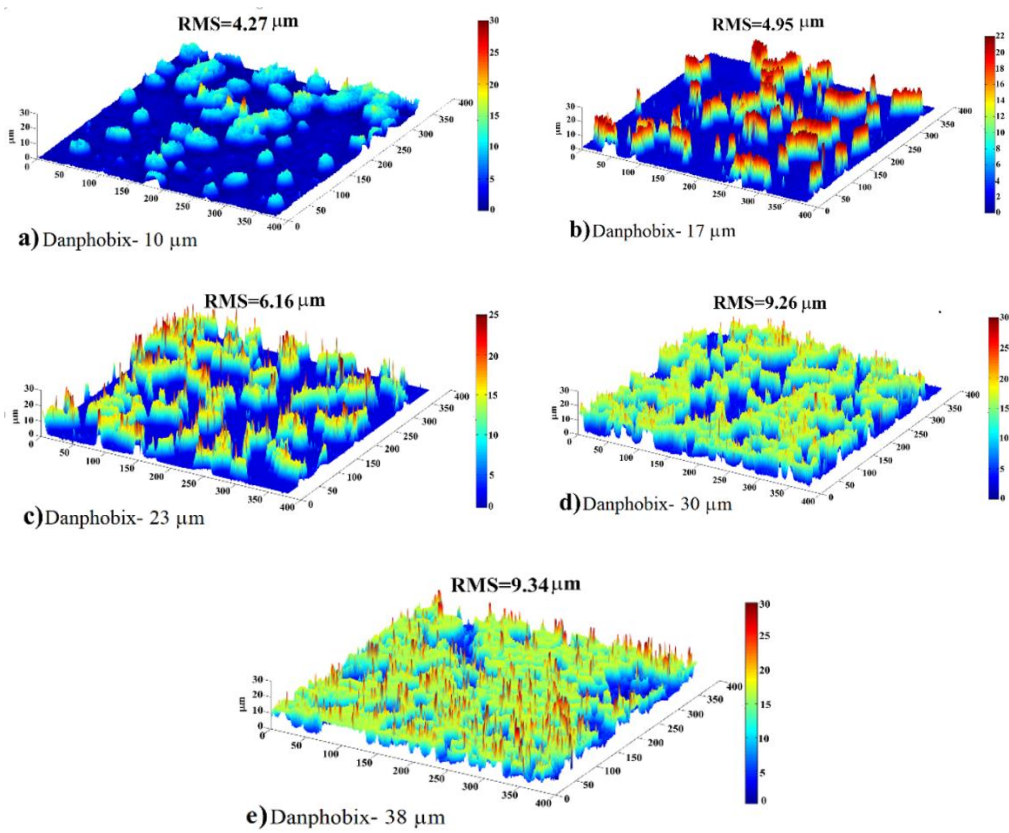


Fig. 7. Surface roughness profiles for Danphobix coatings with thickness of a=10 μm, b=17 μm, c=23 μm, d=30 μm, e=38 μm.

Table 3. Effect of the area coated and coating thickness on the contact angle and contact angle hysteresis.

Test Section	Coating thickness	Percentage of surface coated	Equivalent Coating thickness	Contact Angle	Contact Angle Hysteresis	R _{rms}
	Δl _{Coat} (μm)	A _{Coat} (%)	Δl _{Eq-coat} (μm)	(degree)	(degree)	(μm)
Fig. 7.a	10	54.7	5.47	113±2	58	4.27
Fig. 7.b	17	65.2	11.08	120±2	57	4.95
Fig. 7.c	23	74.7	17.18	123±2	55	6.16
Fig. 7.d	30	82.8	24.84	126±2	53	9.26
Fig. 7.e	38	90.51	34.39	132±3	50	9.34

$$\Delta l_{Eq-coat} = \Delta l_{Coat} \times A_{Coat} \quad (15)$$

Finally, these equivalent thicknesses are used as the thickness of each coating to obtain the surface temperature of the Danphobix coating in the Eq.(5). The values of equivalent thicknesses and surface coverage of Danphobix coatings are shown in Table 3. The contact angle values are also shown in Table 3. According to the measured values, the droplet-surface contact angle increases as the surface coating is enlarged.

Then, the values of CHTC and heat flux was also measured. Fig 8. an indicates the condensation process on the five plates with different coating thicknesses. As can be observed, the diameter of droplets formed on the plates is larger for the lower thickness of coating.

The test was performed in noncontact mode and the root-mean square (RMS) roughness of the films was recorded. The surface morphology of Danphobix coatings was analysed to determine its root-mean square RMS roughness.

Root mean square roughness (R_{rms}) values as formulated in Eq. (14) determined by surface profilometer are given in Table 3 and were found to be in the order of Danphobix-38μm > Danphobix-30μm > Danphobix-23μm > Danphobix-17μm > Danphobix-10μm.

$$R_{rms} = \sqrt{\frac{1}{n} \sum_{i=1}^n y_i^2} \quad (14)$$

The roughness profile contains (n) ordered, equally spaced points along the trace, and (y_i) is the vertical distance (μm) from the mean line. As seen from Fig. 7, Danphobix coatings with thicknesses of 10 μm and 17 μm were flatter than 30 μm and 38 μm and the population of the peaks per unit area (μm²) was largest on the thickness of 38 μm. To better show the surface roughness and its effect on wettability, Fig. 7 is presented. As can be seen, increasing the thickness results in the surface structure decreases the distance between each pick in the roughness meaning less contact angle hysteresis.

The CHTC and heat flux values measured during condensation over the Danphobix coated surfaces are reported in Fig. 8.b and Fig. 8.c, respectively. It

seemed based on the formation of droplets that as the surface thickness increased, the plate hydrophobicity was enlarged as well. The values of heat flux and CHTC was also affected by both the plate coating thickness and hydrophobicity.

Trends are those expected during condensation. The CHTC tends to decrease when increasing subcooling temperature. Instead, heat flux increases when increasing ΔT. On the other hand, the effect of coating thickness on the amount of heat flux and CHTC is such that by decreasing the thickness from 38μm to 17μm, it decreases the heat transfer resistance and consequently increases the heat flux and CHTC values with respect to Fig. 8.b and Fig. 8.c. Also, in spite of the thickness reduction from 17 μm to 10μm, the coating was damaged and CHTC decreased due to the direct steam contact with the plate since the physical structure of surface with the thickness of 10μm was not durable at 100°C. It is worth noting that the heat flux and CHTC values of the plate with 17μm coating was enlarged by 1.97-2.14 times and 1.96-2.46 times compared to the non-coated plate, respectively.

The hydrophobic-hydrophilic hybrid surface can be effectively applied to enhance the condensation heat transfer of steam under low surface subcooling degree and for the condensing surface with larger contact angle hysteresis or smaller contact angle (Peng *et al.* 2014). Figure 8 and Table 3 indicates also that steam condensation heat transfer characteristics such as heat flux and CHTC on hybrid surface with Danphobix coating, enhanced with increase and decrease of contact angle hysteresis and contact angle, respectively.

According to the amounts surface coverage of Danphobix coatings shown in Table 3, increasing the coating thickness, a larger area of the plate was coated with Danphobix. Moreover, the maximum value of CHTC that was obtained at the coating thickness of 17 μm comprised 65.2% of the surface coating by Danphobix.

Among the main conclusions, one can mention that slightly higher condensation rates were obtained for some test sections that had 65.2% of its surface area coated with a Danphobix layer. According to Fig. 6, one of the reasons for better condensation at this plate is the better connection of hydrophilic areas

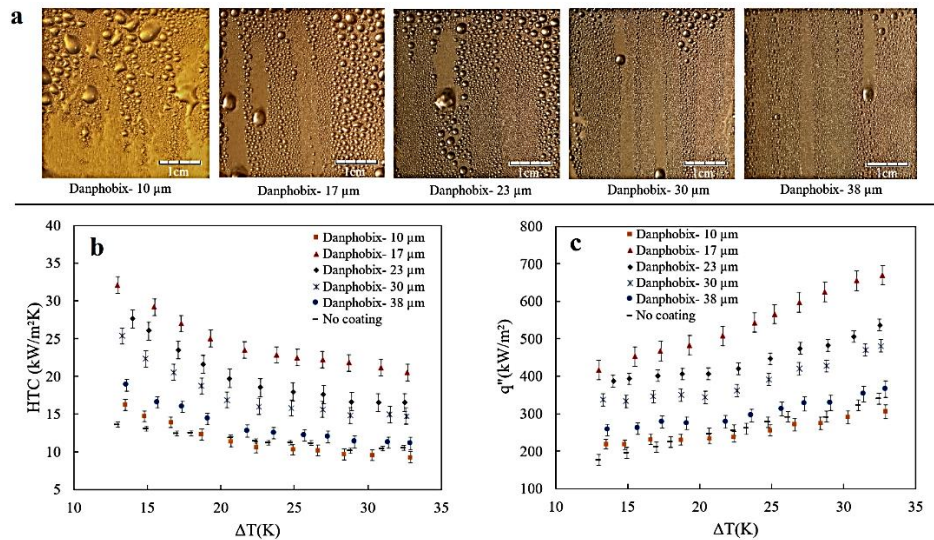


Fig. 8. Condensation on the Danphobix-coated surfaces at five different thicknesses; CHTC (b) and Heat flux (c) versus various subcooling temperatures on the Danphobix-coated surfaces at five different thicknesses.

with each other than plates with coating thicknesses of 23-38 μm , which increases the condensation rate. On the other hand, despite the fact that more hydrophilic areas are connected to each other at a thickness of 10 μm , but because this amount of coating thickness was not durable enough during the condensation test, the surface with a thickness of 17 μm is introduced as the optimal surface.

4. CONCLUSION

The performed measurements of the contact angle, CHTC and heat flux on eight hydrophilic, hydrophobic and superhydrophobic plates were investigated for different coatings. Although the available superhydrophobic coatings had large contact angles, they suffered from poor durability against steam. According to the results, the hydrophobic-hydrophilic coating Danphobix has high durability and higher CHTC and heat flux compared to the other surfaces. Then, five Danphobix-coated plates were generated with the coating thicknesses of 10, 17, 23, 30, and 37 μm . The CHTC of the plate with 17 μm coating was enlarged by more 200% compared to the non-coated plate approximately. In addition, increasing the coating thickness, a larger area of the plate was coated with Danphobix and the maximum value of CHTC that was obtained at the coating thickness of 17 μm included 65.2% of the surface coating by Danphobix.

ACKNOWLEDGEMENTS

The authors would like to thank the members of the Institute of Applied Hydrodynamics and marine technology of Iran University of Science and Technology (Hydrotech), Dr. Setareh Sekhavat, Eng. Ali Ansari, Dr. Mohammad Saadat Bakhsh, Eng. Ehsan Dehnavi and Eng. Shahin Jamali Asl for their collaboration for producing coatings in the work.

REFERENCES

- Ansari, A. (2017). *Experimental evaluation of antifouling superhydrophobic coating*. MSc Thesis, Iran university of science and technology.
- Baojin, Q., Z. Li, X. Hong and S. Yan (2011). Experimental study on condensation heat transfer of steam on vertical titanium plates with different surface energies. *Experimental Thermal and Fluid Science* 35, 211–218.
- Beér, J. M. (2007). High efficiency electric power generation: The environmental role. *Progress in Energy and Combustion Science* 33, 107–134.
- Chatterjee, A., M. M. Derby, Y. Peles and M. K. Jensen (2013). Condensation heat transfer on patterned surfaces, *International Journal of Heat Mass Transfer* 66, 889–897.
- Chatterjee, A., M. M. Derby, Y. Peles and M. K. Jensen (2014). Enhancement of condensation heat transfer with patterned surfaces, *International Journal of Heat Mass Transfer* 71, 675– 681.
- Citakoglu, E. and J. W. Rose (1968). Dropwise condensation-some factors influencing the validity of heat-transfer measurements. *International Journal of Heat Mass Transfer* 11(3), 523-537.
- Derby, M. M., A. Chatterjee, Y. Peles and M. K. Jensen (2014). Flow condensation heat transfer enhancement in a mini-channel with hydrophobic and hydrophilic patterns, *International Journal of Heat Mass Transfer* 68, 151–160.
- Ghosh, A., S. Beaini, B. J. Zhang, R. Ganguly, C. and M. Megaridis (2014). Enhancing

- Dropwise Condensation through Bioinspired Wettability Patterning, *Langmuir* 30, 13103-13115.
- ISO Guide to the Expression of Uncertainty in Measurement, (1995).
- Izumi, M., S. Kumagai, R. Shimada and N. Yamakawa (2004). Heat transfer enhancement of dropwise condensation on a vertical surface with round shaped grooves. *Experimental Thermal and Fluid Science* 49(2), 243-248.
- Ji, X., D. Zhou, C. Dai and J. Xu (2019). Dropwise condensation heat transfer on superhydrophilic-hydrophobic network hybrid surface. *International Journal of Heat Mass Transfer* 132, 52-67.
- Khawaji, A. D., I. K. Kutubkhanah and J. M. Wie (2008). Advances in seawater desalination technologies, *Desalination* 221 (1), 47–69.
- Koch, G., D. C. Zhang and A. Leipertz (1997). Condensation of steam on the surface of hard coated copper discs. *Heat Mass Transfer* 32(22), 149-156.
- Lemmon, NIST Standard Reference Database 23: Reference Fluid Thermodynamic and Transport Properties-REFPROP, Version 9.1.
- Liu, L. and A. M. Jacobi (2006). The Effects of Hydrophilicity on Water Drainage and Condensate Retention on Air-Conditioning Evaporators. *International Refrigeration and Air Conditioning Conference*, paper 847.
- Majumdar, A. and I. Mezic (1999). Instability of ultra-thin water films and the mechanism of droplet formation on hydrophilic surfaces. *Journal of Heat Mass Transfer* 121(4), 964-971.
- Oestreich, J. L., C. W. M. van der Geld, J. L. G. Oliveira and A. K. da Silva (2019). Experimental condensation study of vertical superhydrophobic surfaces assisted by hydrophilic constructal-like patterns. *International Journal of Thermal Sciences* 135, 319–330.
- Parin, R., D. Del Col, S. Bortolin and A. Martucci (2016). Dropwise condensation over superhydrophobic aluminium surfaces. *Journal of Physics: Conference Series* 745(032134).
- Peng, B., X. Ma, Z. Lan, W. Xu and R. Wen (2015). Experimental investigation on steam condensation heat transfer enhancement with vertically patterned hydrophobic–hydrophilic hybrid surfaces. *International Journal of Heat Mass Transfer* 83(4), 27-38.
- Peng, B., X. Ma, Z. Lan, W. Xu and R. Wen (2014). Analysis of condensation heat transfer enhancement with dropwise-filmwise hybrid surface: Droplet sizes effect. *International Journal of Heat Mass Transfer* 77, 785–794.
- Peters, T. B., M. McCarthy, J. Allison, F. A. Dominguez-Espinosa, D. Jenicek, H. A. Kariya, W. L. Staats, J. G. Brisson, J. H. Lang and E. N. Wang (2012). Design of an Integrated Loop Heat Pipe Air-Cooled Heat Exchanger for High Performance Electronics. *IEEE Transactions on Components, Packaging and Manufacturing Technology* 2, 1637–1648.
- Schmidt, E., W. Schurig and W. Sellschopp (1930). Condensation of water vapor in film and drop form. *Zeitschrift Des Vereines Deutscher Ingenieure* 74, 544-544.
- Tianqing, L., M. Chunfeng, S. Xiangyu and X. Songbai (2007). Mechanism study on formation of initial condensate droplets. *The American Institute of Chemical Engineers Journal* 53(4), 1050–1055.
- Vemuri, S. and K. J. Kim (2006). An experimental and theoretical study on the concept of dropwise condensation. *International Journal of Heat Mass Transfer* 49(3), 649-657.
- Zhao, Z.N. (2003). *Heat Transfer*, Higher Education Press, Beijing.